PHASE FIELD MODELING OF NEAR-WELLBORE HYDRAULIC FRACTURE NUCLEATION AND PROPAGATION

Organization:	University of Utah
Recipient Organization:	Lawrence Livermore National Laboratory
DUNS Number:	009095365
Recipient Address:	7000 East Ave. Livermore, CA 94550

Award Number:	2-2446
Project Title:	Closing the loop between in situ stress complexity and EGS fracture complexity
Project Period:	10/01/2021 – 06/30/2025

Principal Investigator(s):	Matteo Cusini (PI) cusini1@llnl.gov Andrew Bunger (Co-PI) bunger@pitt.edu
Report prepared by:	Fan Fei (LLNL) Matteo Cusini (LLNL)
Report Submitted by:	Matteo Cusini

Date of Report Submission:	February 5, 2024
Related milestones:	MILESTONE 2.1.1

This work was performed under the auspices of the U.S. Department of Energy by Lawrence Livermore National Laboratory under Contract DE-AC52-07NA27344.

PHASE-FIELD MODELING OF NEAR-WELLBORE HYDRAULIC FRACTURE NUCLEATION AND PROPAGATION

1.1 Introduction

The goal of *Task 2* of the project titled "Closing the loop between in situ stress complexity and EGS fracture complexity" is to model fracture nucleation and propagation in the near wellbore region and, in combination with the experimental study conducted as part of *Task 4*, investigate the relationship between the in situ stress and the near-wellbore fracture patterns. To this end, We have identified phase field as a promising modeling approach to model the nucleation and propagation process in the near wellbore region. In phase field, fractures are represented by a diffuse variable, i.e the damage. Compared to approaches that model fractures as sharp interfaces, phase field does not require any re-meshing or element insertion algorithm, which makes the treatment of complex fracture geometries straightforward, even with simple meshes.

On the other hand, all phase field formulations for hydraulic fracturing that had been developed prior to the start of this project, focused on the propagation of existing fractures. In fact, they cast the problem in terms of the minimization of the total potential energy of the system. As a consequence, they accurately model fracture propagation, in agreement with fracture mechanics theory, but they neglect the material strength-based mechanism that determines fracture nucleation in the bulk of the material. Thus, we have devised a novel phase field formulation for hydraulic fracturing capable of modeling both nucleation and propagation. Specifically, we have extended the work by Kumar et al. (2020), which focuses on traction-free fractures in brittle materials, to hydraulic fracturing and we have implemented our novel formulation in the GEOS simulation framework.

In this report, we provide a brief description of the phase field formulation we have developed in Section 1.2. Then, in Section 1.3, we summarize the discretization and the solution strategy that we have adopted in GEOS. Finally, in Section 1.4 we present some numerical examples of near-wellbore hydraulic fracturing, both 2D and 3D, to demonstrate how phase field can be used to model the systems of interest. Finally, in Section 1.5, we draw some conclusion and discuss future steps.

1.2 phase field approximation and governing equations

Let us consider a poroelastic domain Ω fully saturated by a compressible fluid. The domain boundary, $\partial\Omega$, consists of a displacement boundary $\partial_u\Omega$, a traction boundary $\partial_t\Omega$, a pressure boundary $\partial_p\Omega$ and a flux boundary $\partial_q\Omega$, such that

$$\partial_u\Omega \cup \partial_t\Omega = \partial\Omega, \quad \partial_u\Omega \cap \partial_t\Omega = \emptyset, \tag{1}$$

$$\partial_p\Omega \cup \partial_q\Omega = \partial\Omega, \quad \partial_p\Omega \cap \partial_q\Omega = \emptyset. \tag{2}$$

Hydraulic fractures Γ may nucleate and evolve inside the domain. To model hydraulic fracturing we seek the displacement u, the pressure p, and the fracture geometry Γ that satisfy the governing equations describing the evolution of the system in the time interval $[0, T]$.

The phase field regularization consists in approximating the hydraulic fractures Γ with a diffusely distributed damage variable $d \in [0, 1]$, where $d = 0$ indicates a fully intact material and $d = 1$ is a completely damaged (fractured) material. Given this regularization, the strong form of the boundary value problem entails finding the displacement ($\boldsymbol{u}$), the fluid pressure (p), and the damage field (d) that satisfy

$$\nabla \cdot [\boldsymbol{\sigma}'(\boldsymbol{\varepsilon}, d) - m(d)(b-1)p\mathbf{1}] - m(d)\nabla p + \rho\boldsymbol{g} = \mathbf{0}, \tag{3}$$

$$\begin{cases} 2(d-1)W^e - m'(d)bp\nabla\cdot\boldsymbol{u} + m'(d)\nabla\cdot(p\boldsymbol{u}) + \dfrac{3\mathcal{G}_c}{8L}\left[1 - 2L^2\nabla d\right] + c_e = 0, \ d > 0, \\ 2(d-1)W^e - m'(d)bp\nabla\cdot\boldsymbol{u} + m'(d)\nabla\cdot(p\boldsymbol{u}) + \dfrac{3\mathcal{G}_c}{8L}\left[1 - 2L^2\nabla d\right] + c_e \leq 0, \ d = 0, \end{cases} \tag{4}$$

$$\frac{\partial}{\partial t}\left(\phi\rho_f\right) + \nabla\cdot\left(\rho_f\boldsymbol{v}\right) = s, \tag{5}$$

subject to the appropriate boundary and initial conditions. Here, Eq. (3) is the momentum balance equation where $\boldsymbol{\sigma}'$ is the effective stress tensor, $\boldsymbol{\varepsilon}$ is the strain tensor, $m(d)$ is a damage-dependent function, b is the rock Biot's coefficient, and $\rho\boldsymbol{g}$ is the body force. Eq. (4) is the damage evolution equation. $W^e(\boldsymbol{\varepsilon})$ is the strain energy of the intact material, $\mathcal{G}_c$ is the critical fracture energy, L is a characteristic length scale, and $c_e(\boldsymbol{\sigma}', L)$ is an external driving force term characteristic of the material strength surface, first introduced in Kumar et al. (2020). Finally, Eq. (5) in which ϕ is the rock porosity, ρ_f is the fluid density, s is the source/sink term and, $\boldsymbol{v}$ is the fluid Darcy's velocity, i.e.

$$\boldsymbol{v} = -\frac{\boldsymbol{k}}{\mu_f}\cdot(\boldsymbol{\nabla}p - \rho_f\boldsymbol{g}). \tag{6}$$

Here, $\boldsymbol{k}$ is the permeability tensor, μ_f is the fluid viscosity. One complexity associated with modeling hydraulic fractures with phase field is the computation of the crack aperture which is challenging when using a diffuse crack representation (see Yoshioka et al. (2020) for more

details). Here, we employ an empirical relationship expressing permeability as a function of damage (Pijaudier-Cabot et al., 2009).

For additional information, we encourage interested readers to consult our detailed publication (Fei et al., 2023a).

1.3 Discretization and solution strategy

Equations (3) - (5) are discretized in time and space. For the time discretization we employ a Euler backward scheme. For the spatial discretization we employ a low order finite element method to discretize the momentum balance and the damage evolution equations whereas we use a hybrid mimetic finite difference scheme to discretize the fluid flow equation.

The nonlinear system of discrete equations (3) - (5) is solved using a sequentially coupled approach, widely used in the phase field literature (e.g., Miehe et al. (2010); Fei and Choo (2021); Geelen et al. (2019)). Given the solution at a given time step n, $\{p^n, u^n, d^n\}$, first, all damage dependencies are frozen and the coupled momentum balance and fluid flow equations are solved to find $p^{\nu+1}$ and $u^{\nu+1}$. Subsequently, with the newly updated values of pressure and displacements, we solve the damage evolution equation to determine $d^{\nu+1}$. This staggered approach is iteratively executed until the solution converges according to a predefined criterion, thereby obtaining the solution at time step $n+1$, i.e. $\{p^{n+1}, u^{n+1}, d^{n+1}\}$.

1.4 Numerical examples

1.4.1 Verification examples

The formulation and discretization methods outlined in the preceding sections have been rigorously verified against analytical solutions. While these verification examples are not included in this report, they can be found in detail in our publications, Fei et al. (2023b) and Fei et al. (2023a).

1.4.2 Near-wellbore hydraulic fracturing examples

In this subsection, we showcase a variety of numerical examples for both two-dimensional (2D) and three-dimensional (3D) models. These examples illustrate the application of our newly developed phase field method in simulating the onset and development of hydraulic fractures near wellbores. We pay particular attention to varying stress conditions and the impact of heterogeneous material property distributions.

The test cases we present here are aligned with the length scales of the experimental setup created for *Task 4* of this project. We have summarized the fluid and rock parameters used in all simulations in Table 1. In our models, we assume materials have no initial deformation ($\varepsilon_{\text{vol},0} = 0$), start with zero fluid pressure ($p_0 = 0$), and exclude gravitational effects which are negligible at the length scales considered.

Bulk modulus, κ	GPa	16.7
Shear modulus, G	GPa	12.5
Critical fracture energy, $\mathcal{G}_c$	kJ/mm^2	0.004
Tensile strength, σ_{ts}	MPa	5.5
Compressive strength, σ_{cs}	MPa	40
Bulk modulus of the grain, κ	GPa	83.5
Matrix permeability, k	m^2	1×10^{-15}
Initial Porosity, ϕ_0	-	0.1
Fluid viscosity, μ_f	cp	1
Fluid density, ρ_f	kg/m^3	1000
Damage coefficient for permeability, α_k	-	7

Table 1: Parameters for the phase field modeling of near-wellbore hydraulic fracturing.

Example 1: near-wellbore nucleation and propagation in 2D

Let us consider a two-dimensional square domain measuring 200 mm on each side, featuring a circular wellbore with an 8 mm diameter located at its center. To mimic the effect of defects on the wellbore surface in our model, we introduce two weak points on the wellbore, as illustrated in Fig. 1. This is accomplished by assigning a lower tensile strength (σ_{ts} = 2 MPa) at these points, which is intended to facilitate fracture nucleation in these areas. This modification enables us to investigate the nucleation of fractures from the wellbore under varying stress conditions. Specifically, we focus on how fractures develop for different ratios of maximum and minimum horizontal stresses.

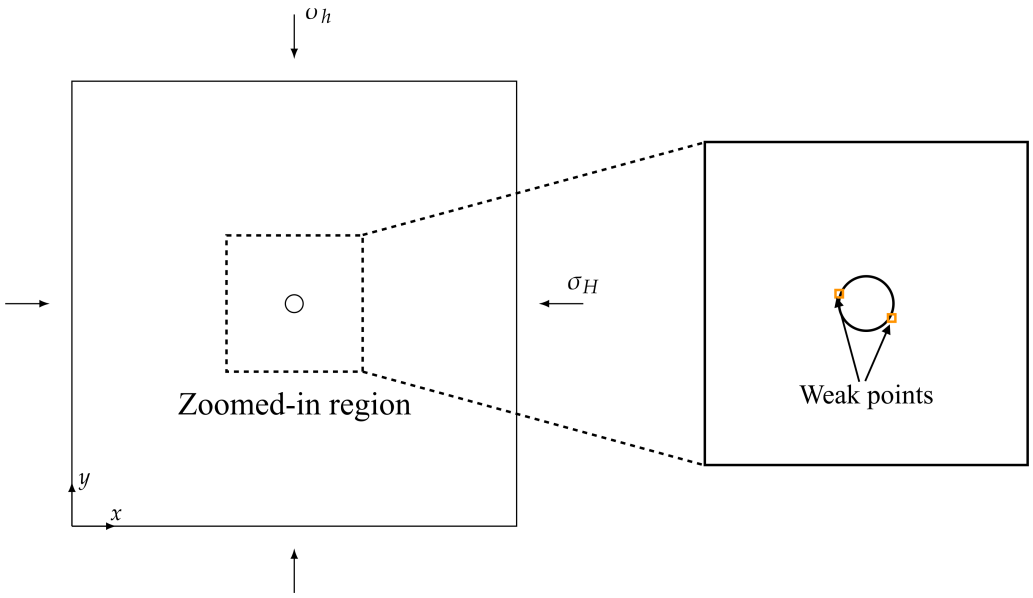

Figure 1: Example 1 - geometry boundary conditions and zoom ono the wellbore surface.

Figure 2 showcases the patterns of near-wellbore hydraulic fractures under a constant minimum horizontal stress (σ_h = 9 MPa) and varying values of the maximum horizontal stress (σ_H). Notably, it becomes apparent that the likelihood of fracture nucleation at the weak points decreases and the fractures tend to orient more perpendicularly to σ_h as the value of σ_H significantly exceeds σ_h. This phenomenon occurs because a larger contrast in horizontal stresses (*i.e.*, $\sigma_H - \sigma_h$) results in a higher tensile stress around the wellbore. As a consequence, the in situ stress exerts a more pronounced influence on the orientation of the near-wellbore hydraulic fractures. Additionally, for the cases with lower values of the maximum horizontal stress (σ_H), fractures tend to realign with the principal direction as they propagate away from the wellbore. Such patterns are consistent with experimental hydraulic fracturing studies (see, e.g., Bunger and Lecampion (2017)).

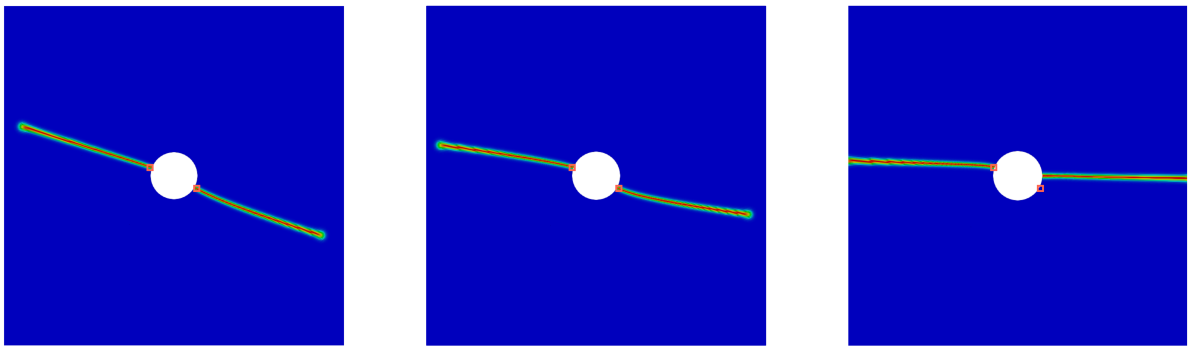

$\sigma_h = 9$ MPa and $\sigma_H = 10$ MPa | $\sigma_h = 9$ MPa and $\sigma_H = 12$ MPa | $\sigma_h = 9$ MPa and $\sigma_H = 15$ MPa

Figure 2: Example 1 - hydraulic fracture patterns obtained for increasing (left to right) values of the maximum horizontal stress.

Example 2: fracture nucleation and propagation from a vertical wellbore

We now shift our focus to a three-dimensional cubic domain, with dimensions of 200 mm on each side. Within this domain, a vertical cylindrical wellbore, which has a diameter of 26 mm and runs parallel to the z-axis, is drilled through. The specific geometry and boundary conditions of this setup are illustrated in Fig. 3. In this model, in situ stresses are applied in all three directions: $\sigma_v = 17.5$ MPa (vertical stress), $\sigma_H = 15$ MPa (maximum horizontal stress), and $\sigma_h = 10$ MPa (minimum horizontal stress). Mirroring the approach used in our previous two-dimensional case, we set zero pressure conditions on all external boundaries of the 3D model and fix their normal displacements. The simulation focuses on the nucleation and growth of hydraulic fractures resulting from fluid being injected at a pressure that increases over time, defined as $p_{\text{inj}}(t) = 1$ [MPa/s]$\cdot t$ [s]. Injection occurs in the central 100 mm section of the wellbore. For this simulation, the regularization length, denoted as L, is set at 1 mm, and the calibrated parameter δ^L has a value of 3.28.

In addition to the previous parameters, our simulation also accounts for a heterogeneous distribution of critical fracture energy as shown in Fig. 4. This mimics the varying resistance to fracture growth across the domain due to the texture of the rock. Furthermore, we have designated three distinct zones along the wellbore, each characterized by a reduced tensile strength. This setup is intended to simulate potential defects on the wellbore surface that may influence the initiation of fractures.

Figure 5 illustrates the evolution of damage in both two-dimensional (at $z = 100$ mm) and three-dimensional views. In the 2D view, it's observed that hydraulic fractures initially nucleate from the two upper weak zones, followed by the formation of a third fracture from the lower one. This pattern echoes the results seen in the 2D wellbore simulations, where fractures exhibit a

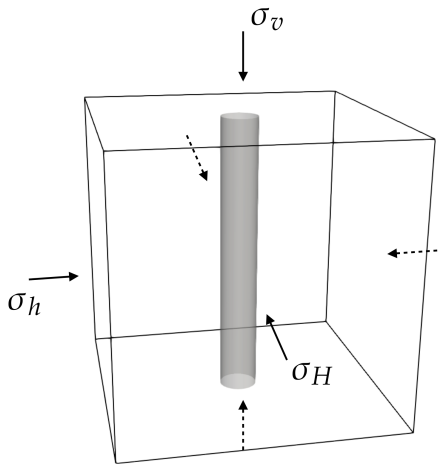

Figure 3: Example 2 - geometry of the 3D wellbore hydraulic fracturing test case.

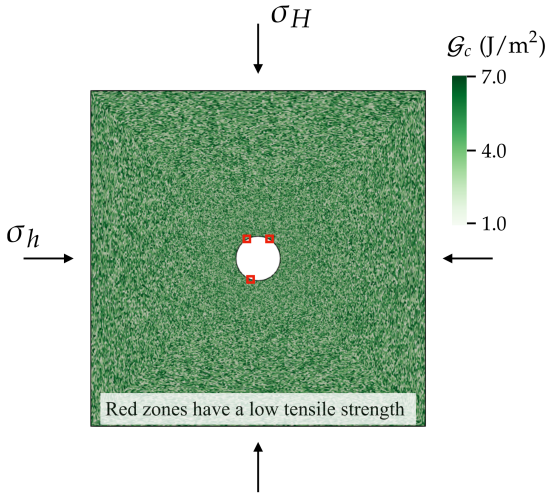

Figure 4: Example 2 - 2D view of the distribution of critical fracture energy.

curved trajectory as they move away from the wellbore. The 3D view further reveals that the fractures do not align with the wellbore's vertical orientation but display slight bending due to the material heterogeneity. This results in more complex fracture patterns in the vicinity of the wellbore.

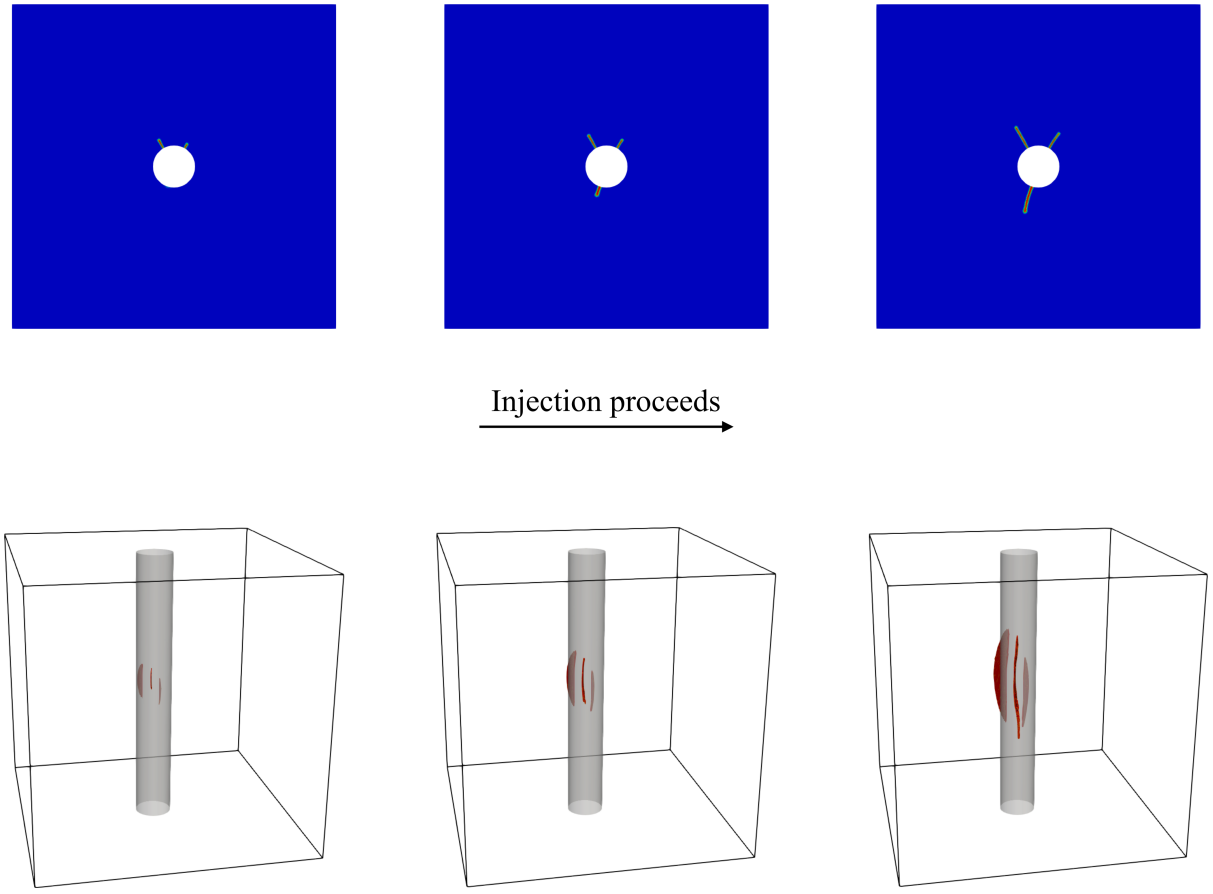

Figure 5: Example 2 - damage evolution representing hydraulic fracture growth from a 3D wellbore with three weak zones and material heterogeneity.

Figure 6 shows, instead, a comparison of the fracture geometries obtained for two different values of the maximum horizontal stress. Remark that as the difference between the minimum and the maximum horizontal stresses increases, there is a marked tendency for fractures to nucleate and extend in the direction perpendicular to σ_h.

1.5 Conclusions and future work

In this report, we have presented the novel phase field formulation we have developed to simulate nucleation and propagation of hydraulic fractures in the near-wellbore region. It is worth underlying the following points:

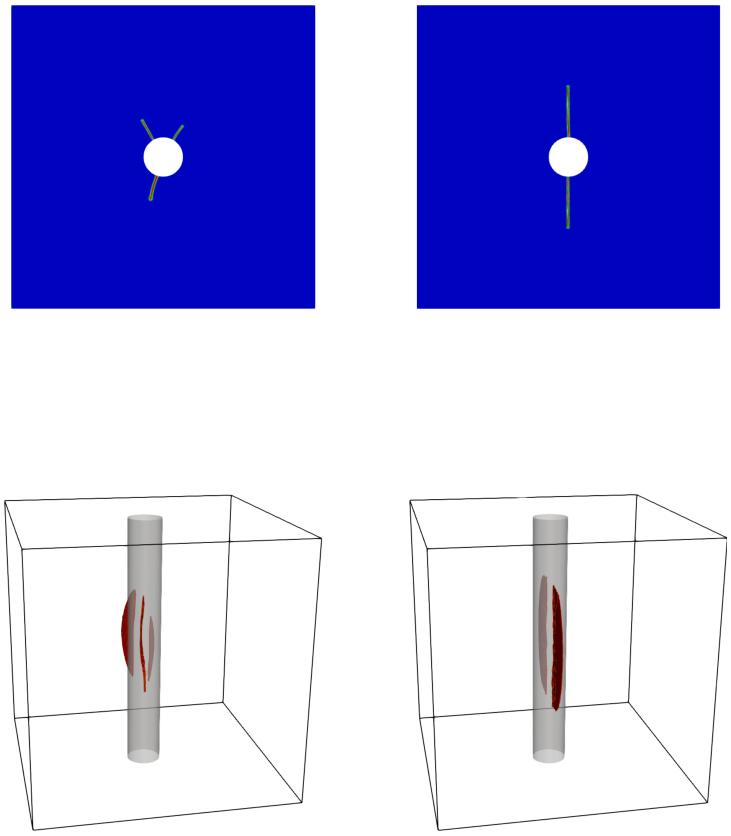

Figure 6: Example 2 - Comparison of the fracture patterns obtained with two different values of the maximum horizontal stress and $\sigma_h = 10$ MPa.

- to correctly capture fracture nucleation, we extended the damage evolution equation by adding the contribution of an external driving force and we have devised the appropriate damage function, $m(d)$;
- we have verified the accuracy of the proposed method with analytical benchmarks;
- as shown by the examples presented, the phase field formulation we have proposed can easily be used to simulate both nucleation and propagation of hydraulic fractures and it can easily deal with complex fracture geometries without the need for complex re-meshing algorithms. As such, it is suited to study the interplay between material heterogeneities, in situ stress, and wellbore orientation on the fracture pattern in the near wellbore region;
- the external driving force term plays a crucial role in our simulations and must be precisely formulated to align with the characteristics of each specific yield surface. Up to this point,

our approach has involved using a version of the external driving force that is specifically designed to complement the Drucker–Prager yield model.

Our ongoing and future efforts are directed towards applying the method we have presented here in conjunction with the hydraulic fracturing experiments carried out under *Task 4* of our project. Additionally, we are planning to expand the scope of our phase field formulation to include non-isothermal conditions, thereby broadening its applicability and relevance in simulating more complex scenarios where temperature variations play a significant role.

Model availability

All results showcased in this report were generated utilizing GEOS, an open-source subsurface simulator available at geos.dev. The GEOS codebase along with all input files used to run the models presented can be accessed and downloaded from its official website at www.geos.dev.

References

Bunger, A., & Lecampion, B. (2017). Four critical issues for successful hydraulic fracturing applications. *Rock mechanics and engineering*(BOOK_CHAP).

Fei, F., & Choo, J. (2021). Double-phase-field formulation for mixed-mode fracture in rocks. *Computer Methods in Applied Mechanics and Engineering*, *376*, 113655.

Fei, F., Costa, A., Dolbow, J. E., Settgast, R. R., & Cusini, M. (2023a). A phase-field model for hydraulic fracture nucleation and propagation in porous media. *International Journal for Numerical and Analytical Methods in Geomechanics*, *47*(16), 3065-3089. Retrieved from https://onlinelibrary.wiley.com/doi/abs/10.1002/nag.3612 doi: https://doi.org/10.1002/nag.3612

Fei, F., Costa, A., Dolbow, J. E., Settgast, R. R., & Cusini, M. (2023b, 03). *Phase-Field Simulation of Near-Wellbore Nucleation and Propagation of Hydraulic Fractures in Enhanced Geothermal Systems (EGS)* (Vols. Day 2 Wed, March 29, 2023). Retrieved from https://doi.org/10.2118/212251-MS doi: 10.2118/212251-MS

Geelen, R. J., Liu, Y., Hu, T., Tupek, M. R., & Dolbow, J. E. (2019). A phase-field formulation for dynamic cohesive fracture. *Computer Methods in Applied Mechanics and Engineering*, *348*, 680-711. Retrieved from https://www.sciencedirect.com/science/article/pii/S0045782519300519 doi: https://doi.org/10.1016/j.cma.2019.01.026

Kumar, A., Bourdin, B., Francfort, G. A., & Lopez-Pamies, O. (2020). Revisiting nucleation in the phase-field approach to brittle fracture. *Journal of the Mechanics and Physics of Solids*, *142*, 104027.

Miehe, C., Welschinger, F., & Hofacker, M. (2010). Thermodynamically consistent phase-field models of fracture: Variational principles and multi-field fe implementations. *International Journal for Numerical Methods in Engineering*, *83*(10), 1273–1311.

Pijaudier-Cabot, G., Dufour, F., & Choinska, M. (2009). Permeability due to the increase of damage in concrete: From diffuse to localized damage distributions. *Journal of engineering mechanics*, *135*(9), 1022–1028.

Yoshioka, K., Naumov, D., & Kolditz, O. (2020). On crack opening computation in variational phase-field models for fracture. *Computer Methods in Applied Mechanics and Engineering*, *369*, 113210. Retrieved from `https://www.sciencedirect.com/science/article/pii/S0045782520303959` doi: https://doi.org/10.1016/j.cma.2020.113210